

Enhancing End Stage Renal Disease Outcome Prediction: A Multi-Sourced Data-Driven Approach

Yubo Li, MS¹, Rema Padman, PhD¹

¹ Carnegie Mellon University, Pittsburgh, PA, USA

Abstract

Objective: To improve prediction of Chronic Kidney Disease (CKD) progression to End Stage Renal Disease (ESRD) using machine learning (ML) and deep learning (DL) models applied to an integrated clinical and claims dataset of varying observation windows, supported by explainable AI (XAI) to enhance interpretability and reduce bias.

Materials and Methods: We utilized data from 10,326 CKD patients, combining their clinical and claims information from 2009 to 2018. Following data preprocessing, cohort identification, and feature engineering, we evaluated multiple statistical, ML and DL models using data extracted from five distinct observation windows. Feature importance and SHAP analysis were employed to understand key predictors. Models were tested for robustness, clinical relevance, misclassification errors and bias issues.

Results: Integrated data models outperformed those using single data sources, with the Long Short-Term Memory (LSTM) model achieving the highest AUC (0.93) and F1 score (0.65). A 24-month observation window was identified as optimal for balancing early detection and prediction accuracy. The 2021 eGFR equation improved prediction accuracy and reduced racial bias, especially for African American patients.

Discussion: Improved ESRD prediction accuracy, results interpretability and bias mitigation strategies presented in this study have the potential to significantly enhance CKD and ESRD management, support targeted early interventions and reduce healthcare disparities for this population.

Conclusion: This study presents a robust framework for predicting ESRD outcomes in CKD patients, improving clinical decision-making and patient care through multi-sourced, integrated data and AI/ML methods. Future research will expand data integration and explore the application of this framework to other chronic diseases.

1 Introduction

Chronic Kidney Disease (CKD) is a complex, multi-morbid condition marked by a gradual decline in kidney function, which can ultimately progress to end-stage renal disease (ESRD) [1]. With a global prevalence of CKD ranging from 8% to 16%, and estimates suggesting that around 5-10% of individuals diagnosed with CKD eventually reach ESRD[2], they represent a major public health challenge, particularly due to its strong associations with diabetes and hypertension [3]. CKD progression is classified into five stages, culminating in ESRD, where kidney function drops to 10–15% of normal capacity, necessitating dialysis or transplantation for patient survival [1]. The economic impact of CKD is significant, with a relatively small proportion of Medicare CKD patients in the United States contributing to

a disproportionately high share of Medicare expenses, particularly when they progress to ESRD. Additionally, more than one-third of ESRD patients are readmitted within 30 days of discharge, underscoring the critical need for early detection and management of CKD to prevent its progression to ESRD and to reduce healthcare costs [4].

Previous efforts to predict CKD progression to ESRD have primarily relied on either clinical data from electronic health records (EHRs) [5] or administrative claims data [6, 7]. While informative, these studies often utilize a limited set of features, potentially under-representing the complexity of CKD progression. For instance, Sharma et al. [8] developed a model using claims data to identify CKD patients at risk of Hyperkalemia, and Krishnamurthy et al. [6] predicted CKD onset using comorbidities and medications from Taiwan's National Health Insurance Database. However, claims-based studies generally lack the granularity of clinical data, which offers detailed insights through laboratory results, medication records, and patient demographics. For example, Tangri et al. [9] used clinical variables such as age, gender, estimated glomerular filtration rate (eGFR)[10], and albuminuria to predict ESRD progression, and Keane et al. [11] utilized serum creatinine and urine protein levels for high-risk patient identification. Despite their value, models based solely on clinical data may miss the full spectrum of patient interactions with the healthcare system and often struggle with missing data and inconsistent recording practices. Additionally, they may overlook socio-economic factors and healthcare utilization patterns, limiting their applicability across diverse patient populations.

In the field of explainable AI (XAI) for healthcare, established methods such as SHapley Additive exPlanations (SHAP) [12] and Local Interpretable Model-agnostic Explanations (LIME) [13] have been applied to predict ESRD, laying a strong foundation for enhancing the interpretability of deep learning models. However, relying solely on a single source of data — whether claims or clinical — restricts the ability to fully understand the complexity and variability of CKD progression across a diverse patient population and predict ESRD, thereby limiting the real-world applicability of these models.

This study aims to bridge this gap by developing a robust and comprehensive framework that not only utilizes clinical or claims data in isolation but also harnesses the combined strengths of these integrated data sets. At the same time, by minimizing the observation window needed for accurate prediction, our framework integrates clinical relevance with a practical, patient-centered focus. This approach enhances predictive accuracy and clinical utility, enabling more informed decision-making to ultimately improve patient outcomes.

2 Objective

This research aims to evaluate prediction models for CKD progression to ESRD using an integrated dataset of clinical and claims data. Fig. 1 illustrates the key temporal components of our study design, with the observation window beginning at Stage 3 diagnosis (t=0). During this observation window, patients may progress through different CKD

stages (S4, S5); however, we specifically focus on the cohort that does not develop ESRD within the observation window itself. This ensures that our predictive modeling uses only pre-ESRD data to forecast future ESRD development. Our primary objectives are:

- ESRD Risk Prediction: To estimate the probability that a CKD patient will develop ESRD in the future, based on data from a specified observation window that begins from each patient's first occurrence of CKD stage 3.

This probability is represented as:

$$P(\text{ESRD}_i = 1 \mid t > t_{\text{obs}}, X_{\text{clinical},i}(t_{\text{obs}}), X_{\text{claim},i}(t_{\text{obs}})),$$

where $X_{\text{clinical},i}(t_{\text{obs}}), X_{\text{claim},i}(t_{\text{obs}})$ denote the clinical and claims data observed up to time t_{obs} for patient i .

- Observation Window Optimization: To identify the optimal observation window T_{obs} that provides the best performance across all candidate windows t_{obs} (6, 12, 18, 24, and 30 months), ensuring accurate predictions while minimizing the length of the observation window required:

$$T_{\text{obs}} = \arg \max_{t \in \{6, 12, 18, 24, 30\}} \text{Performance}(t),$$

where $\text{Performance}(t)$ is evaluated based on key predictive metrics: F1-score (the harmonic mean of precision and recall) [14], Area Under the Receiver Operating Characteristic curve (AUROC) [15], and Area Under the Precision-Recall Curve (AUPRC) [16].

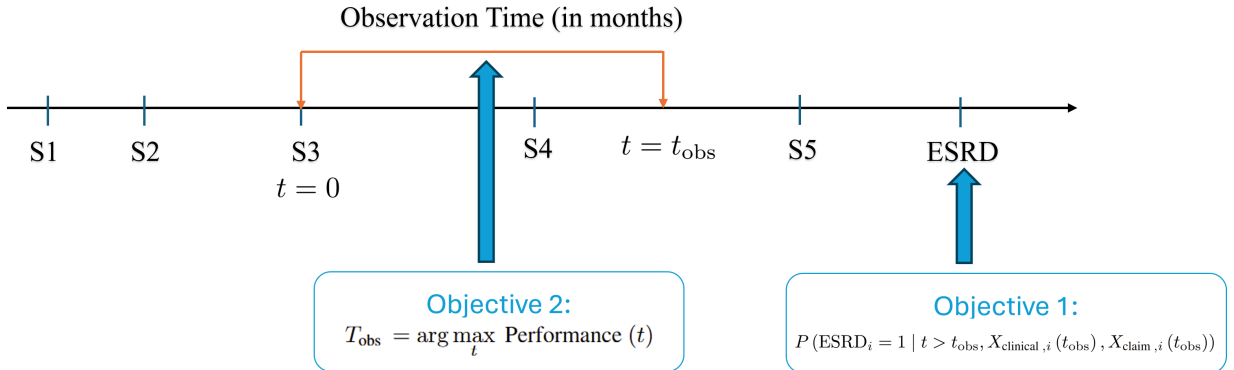


Figure 1: A timeline illustration of observation windows for CKD progression to ESRD. The observation starts at CKD Stage 3. Objective 1 estimates the probability of ESRD occurrence using clinical and claims data within the observation window, while Objective 2 identifies the optimal observation window that maximizes predictive performance.

This approach balances the trade-off between maximizing predictive accuracy and minimizing the duration of the observation window required for reliable predictions. Additionally, we apply explainable AI techniques, such as feature importance and SHAP analysis, to enhance model transparency at both the cohort level to identify key factors, and the individual level to provide personalized insights.

3 Data Sources

This study utilized two key de-identified datasets from different healthcare organizations: administrative claims data and clinical data. The de-identified administrative claims dataset was provided by Highmark, a major health insurance provider, and includes patient interactions with healthcare professionals from January 1, 2009, to December 31, 2018. This dataset encompasses diagnosis codes, treatment records, and healthcare costs for individuals diagnosed with CKD. The use of this dataset was approved by Highmark’s Institutional Review Board.

The clinical dataset was sourced from the EHR data of TMA, P.C., a leading community nephrology practice. This dataset contains laboratory results, patient demographics, diagnostic details, and medication records spanning from 1998 to 2018. For consistency of integration, the clinical data was truncated to match the 10-year span of the claims data (2009–2018). Usage of the clinical data was approved by the Institutional Review Board of Carnegie Mellon University.

Preprocessing of the claims data involved removing duplicates, excluding records without any CKD stage information, and eliminating entries with negative costs to ensure data integrity. After cleaning, the claims dataset included 5,317,178 individual claims across 7,129 unique patients. The clinical dataset was similarly refined to include 433,421 laboratory records for 10,326 patients. These datasets were then integrated using unique patient IDs to provide a comprehensive view of each patient’s medical and claims history.

4 Methods

As shown in Figure 7, our approach to predicting Chronic Kidney Disease (CKD) progression to End-Stage Renal Disease (ESRD) encompasses three primary stages: Data Preparation, Modeling and Validation, and Additional Analyses to assess robustness and clinical utility.

4.1 Data Preparation

4.1.1 Data Pre-processing

As mentioned earlier, we performed data cleansing to ensure the integrity of the datasets. This process involved removing duplicate records to prevent redundancy and potential biases in the analysis. We also excluded entries

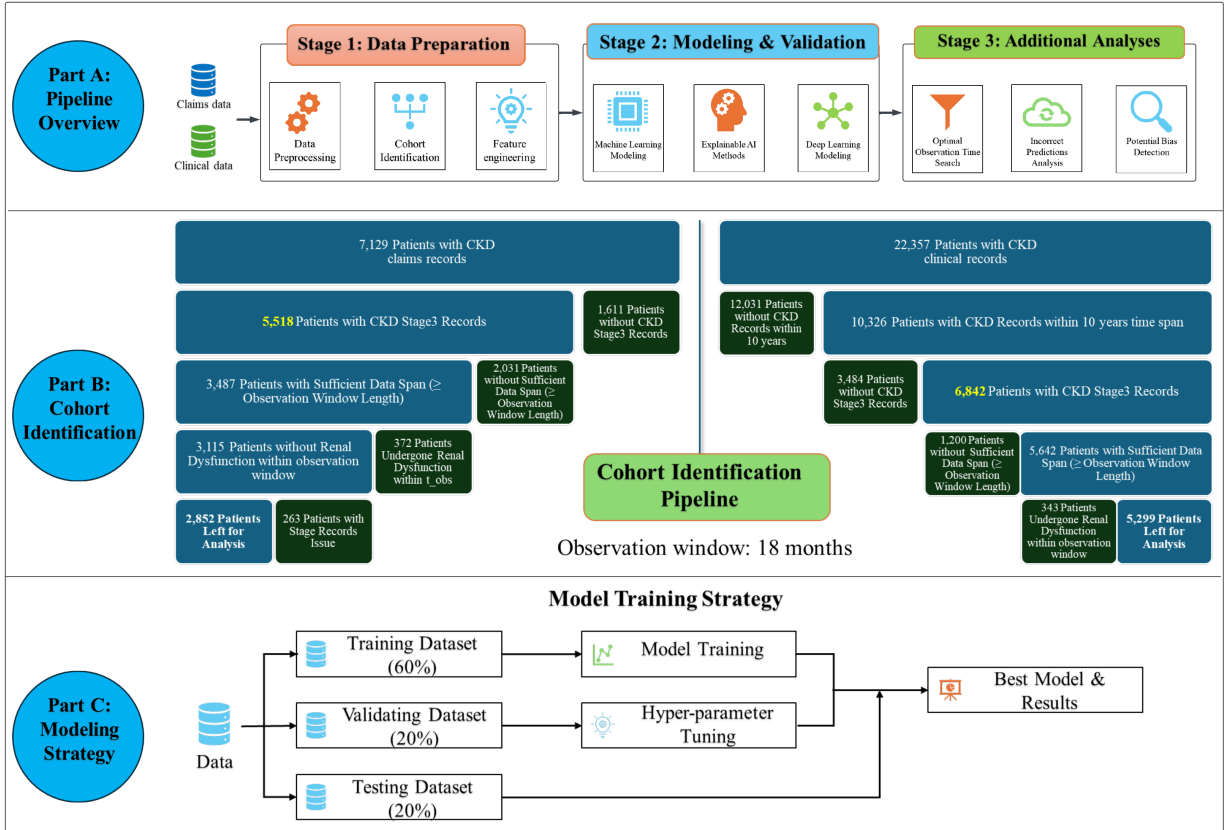


Figure 2: Overview of research framework and training strategy. Part A provides an overview of the data preparation, modeling and validation, and additional analyses pipeline. Part B illustrates the cohort identification process, detailing the inclusion and exclusion criteria applied to claims and clinical records. Part C outlines the modeling strategy.

lacking any stage of CKD diagnoses to maintain the datasets' relevance to our study objectives, and claims records with negative values, which likely indicated data entry errors.

To address missing data issue, we employed Multiple imputation using chained equation (MICE)[17], a widely adopted method in healthcare research for its ability to account for multivariable relationships and provide robust imputations. Normalization was applied to ensure that features contributed proportionately to the analysis. We scaled numerical values to a standard range, a step essential for algorithms sensitive to the magnitude of input values. We applied log transformations [18] to variables exhibiting skewed distributions to stabilize variance and approximate normality. This approach is particularly beneficial for handling data with exponential growth patterns, as it mitigates the impact of outliers and enhances the performance of linear models.

In the laboratory data, we observed an additional challenge where many records lacked unit specifications, leading to significant discrepancies in numerical values. To address this, we conducted distribution detection & adjustment[19] to identify and correct unit inconsistencies. By analyzing the statistical distribution of each laboratory measurement, we detected shifts indicative of differing units. In consultation with clinical experts, we established expected value ranges for each measurement. Outlier values that deviated markedly from these ranges were adjusted to align with the appropriate units, ensuring consistency and comparability across all records.

4.1.2 Cohort Identification

In Part B of Fig.7, cohort identification was conducted to define patient subsets aligned with the research objectives, ensuring that data included full observation windows after CKD stage 3 and excluded those who developed ESRD within this period. Although the example in the figure uses an 18-month observation window, the exact duration may vary based on the selected window of observed data.

The study cohort was further curated through a multi-step process, focusing on patients diagnosed at CKD stage 3 to capture a critical period for potential intervention available to nephrologists. We retained patients with comprehensive data extending beyond the observation window, ensuring a longitudinal view of their CKD management, resulting in a final cohort with uninterrupted, detailed clinical and claims histories.

4.1.3 Feature Engineering

Part C depicted in Fig. 7 involves identifying and creating predictive variables essential for modeling. With claims data, we categorized the features used for prediction into two main groups. The first, cost-based features, was derived from five types of claims: Inpatient, Outpatient, Professional, Pharmacy, and Vision. These features include the count of unique claims per type, the aggregate cost of each type, the range of claim costs, and the standard deviation of claim

costs for each patient.

The second group, comorbidity-based features, includes patient-specific clinical information such as the patient duration in CKD stage 3, the number of emergency department (ED) visits, and the presence of critical comorbidities such as hypertension, diabetes, and phosphatemia.

Clinical data features were categorized into three groups based on consultations with nephrologists, commonly referenced literature, and the characteristics of our datasets. These groups include demographic features, laboratory data features, and comorbidity features.

- Demographic Features: These include age, gender, ethnicity and body mass index (BMI), which have been widely used for understanding CKD progression.
- Laboratory Data Features: This group consists of critical laboratory results such as eGFR, hemoglobin, phosphorus, serum calcium, and bicarbonate, which are important for monitoring CKD. Notably, urine albumin-to-creatinine ratio (UACR) [20] and sodium were not selected due to insufficient readings in the dataset.
- Additional Comorbidity Features: These capture the presence of additional health conditions such as cardiovascular disease, anemia, and metabolic acidosis, in addition to those identified using claims data, and have been shown to influence CKD outcomes.

Following these steps, statistical analyses were performed to compare variables between patients who progressed to ESRD and those who did not. For continuous variables, data were assessed for normality; those meeting normality assumptions were analyzed using independent t-tests to compare group means. For non-normally distributed variables, logarithmic transformations were applied during preprocessing to approximate normality before conducting t-tests. Categorical variables were expressed as frequencies (percentages) and compared using chi-squared tests. Statistical significance was set at $p < 0.05$ for all analyses.

4.2 Modeling & Validation

To develop predictive models for CKD progression to ESRD, we employed both machine learning (ML) and deep learning (DL) frameworks to capture complex data patterns. Our overarching strategy involved partitioning the dataset into training, validation, and testing subsets through stratified sampling, maintaining class distribution across all splits. This approach is particularly crucial in medical research, where class imbalances can significantly impact model performance. To further address the imbalance, we applied SMOTE [21, 22] to the training data, generating synthetic minority samples and enhancing the model's ability to learn from underrepresented classes.

4.2.1 Machine Learning Methods

We employed statistical methods, beginning with logistic regression (LR) [23] as a baseline model to estimate the probability of ESRD progression using clinical and claims data features. Beyond LR, we utilized ML techniques such as Random Forest (RF) [24] and Extreme Gradient Boosting (XGBoost) [25]. We evaluated performance using a standard k-fold cross-validation setup [26]. RF uses ensemble learning by constructing multiple decision trees, which improves model accuracy and mitigates overfitting. XGBoost, a gradient boosting algorithm, builds models iteratively to correct errors from previous iterations, proving highly effective for structured data.

To enhance model interpretability, we conducted cohort-level feature importance analysis to identify key predictors across the dataset. Additionally, SHAP analysis was applied at the individual level to elucidate each feature’s contribution to specific predictions. This dual approach—cohort-level and individual-level analysis—not only provides insights into the drivers of ESRD progression but also improves model transparency, supporting personalized treatment decisions.

4.2.2 Deep Learning Methods

To develop a robust predictive model for CKD progression to ESRD, we followed methodologies from prior studies [7, 27] and constructed a longitudinal data representation segmented into three-month intervals from each patient’s initial CKD stage 3 diagnosis. These three-month intervals are indexed as timestamps (timestamp 0 for months 0-3, timestamp 1 for months 3-6, and so on), with a 18-month observation window containing six timestamps in total. This temporal segmentation approach serves multiple purposes: it captures the temporal evolution of CKD, reflects its gradual progression, and aligns with clinical guidelines for periodic nephrologist visits, while also addressing potential time lags between claims and clinical data. Numerical features were aggregated, categorical features were encoded binarily to capture conditions or events, and a baseline assessment of historical records was conducted to adjust for pre-existing conditions, ensuring the model accurately accounted for CKD presence and progression. This timestamp-based structure enables our model to track the progression of disease markers and identify critical temporal patterns that may indicate increased risk of ESRD development.

We evaluated several deep learning architectures: Convolutional Neural Network (CNN) [28] for feature extraction, Recurrent Neural Network (RNN) [29], Long Short-Term Memory network (LSTMs [30], Gated Recurrent Unit (GRU) [31] for temporal dependency modeling, and Temporal Convolutional Network (TCN) [32] for sequence modeling. These models were chosen to provide a robust foundation for accurately predicting ESRD progression, identifying key risk factors, and anticipating CKD to ESRD transition with high precision. We forgo k-fold cross-validation due to high computational costs and training variance from random initialization[33]. Modern regularization tech-

niques like dropout reduce this need, so we opted for stratified holdout validation to balance efficiency and reliability while maintaining class distributions.

4.2.3 Hyperparameter Tuning

For performance optimization, we employed specialized Python libraries (Python 3.10) to optimize model performance through hyperparameter tuning. For machine learning models, we utilized the H2O framework [34], which provides comprehensive grid search capabilities. The framework systematically explores a predefined set of hyperparameters to identify the optimal combination for model performance. For deep learning models, we leveraged Microsoft's Neural Network Intelligence (NNI) [35]. NNI is an open-source Python toolkit that automates neural architecture search and hyperparameter optimization. It efficiently dispatches and manages trial jobs generated by various tuning algorithms, facilitating the search for optimal neural architectures and hyperparameter configurations.

4.3 Additional Analyses

The comparison of these modeling results helps us identify the optimal observation length and the most reliable and accurate model for predicting CKD progression to ESRD. However, recognizing the limitations of focusing solely on fixed timelines, we extended our analysis to address clinical realities. In practice, the progression timeline from CKD to ESRD is often uncertain when a patient presents for evaluation. To accommodate this variability, we leveraged the selected optimal model and observation window to integrate all time-length cohorts, ranging from 6 to 30 months. This integration enables predictions of ESRD likelihood and optimal observation windows without requiring precise progression timelines, enhancing the model's relevance and applicability in real-world clinical settings. Building on this framework, we conducted additional analyses to further refine the model, including a detailed investigation of misclassifications and their potential causes, as well as an evaluation of the impact of updated eGFR equations on racial bias in CKD predictions. These efforts aim to ensure fairness and accuracy in the model's clinical applications.

4.3.1 Analysis of Model Misclassifications

To evaluate the performance and robustness of our optimal model, we conducted an in-depth analysis of misclassifications by examining predictive probability distributions across the entire sample set. This analysis focused on type 1 (false positive) and type 2 (false negative) errors to understand discrepancies between predicted and actual outcomes. We analyzed instances where the model incorrectly predicted ESRD progression (type 1 error) and where it failed to predict ESRD progression in patients who eventually developed the condition (type 2 error). By comparing these error types, we sought to identify common factors or patterns contributing to misclassification, thus highlighting the model's limitations and suggesting areas for refinement.

This detailed error analysis is crucial for improving the model's accuracy and ensuring its reliability in clinical settings. By understanding the reasons behind incorrect predictions, we can enhance the model's ability to support clinicians in making more informed and accurate decisions regarding patient care.

4.3.2 Impact of Updated eGFR Equations on Racial Bias in CKD Predictions

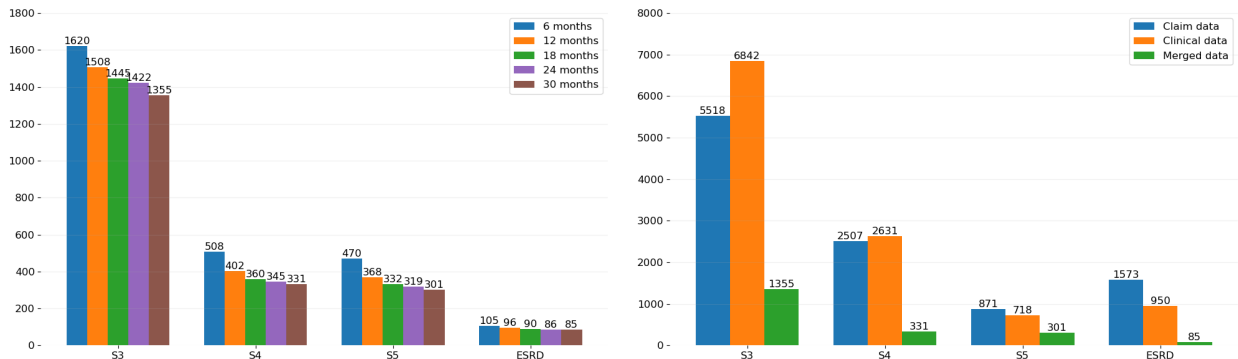
The evolution of eGFR equations has aimed to address inherent limitations, particularly concerning racial bias. In 2020, the use of race-based components in eGFR calculations was scrutinized due to a lack of evidence of its biological basis and the risk of perpetuating racial stereotypes and disparities in healthcare. In response, a 2021 workgroup led by the National Kidney Foundation and American Society of Nephrology recommended an updated CKD Epidemiology Collaboration (CKD-EPI) creatinine equation [36], which excluded the race coefficient to improve accuracy and equity [37]. This adjustment aimed to enhance prediction precision, especially for minority populations [38, 39].

Our analysis, using data from 2009 to 2018, applied both eGFR equations to the data. To assess the impact of the updated equation, we compared predictions between the old and new equations, focusing on improvements in accuracy and equity, particularly for minority groups.

It is important to note that adopting the updated equation may alter the cohort used for analysis, as the new eGFR values directly influence CKD stage classification. This could impact the cohort identification process, and lead to the reclassification of patients, particularly those near stage boundaries. Such changes may affect both the composition of the cohort and the model's predictions.

5 Results

5.1 Cohort for Analysis & Data Characteristics



(a) Variation in CKD stage distribution as a function of different observation window lengths. (b) Comparison of CKD stage distribution across claims, clinical, and merged data with a 30-month observation window.

Figure 3: Overview of CKD Stage Distribution in Merged Data Across Observation Windows.

In this subsection, we present the trends observed during our data integration process and provide a detailed overview

of the data characteristics for the final cohort utilized in our model performance analysis. Fig.3a illustrates the changes in patient distribution across CKD stages over varying observation window lengths. As the observation window extends from 6 to 30 months, there is a gradual decline in the number of patients available for analysis. This decline reflects the exclusion of patients who either lacked sufficient data within the specified window or progressed to ESRD during the period. Additionally, some patient losses may be due to mortality, but we lack the data to confirm this.

To ensure model consistency and fair comparability, we trained and tested on the same cohort. Recognizing the challenge of shrinking cohort size with extended observation windows, we focused on patients with at least 30 months of data following CKD stage 3 diagnosis and split the test data from this group. For the training data, we used the same cohort but with varying data lengths corresponding to the selected observation windows. This approach allowed us to explore the impact of different observation windows and identify the optimal one based on the performance on test data.

After establishing the cohort with at least 30 months of post-CKD stage 3 data, we compared the datasets derived from claims data only (5,518 patients), clinical data only (6,842 patients), and the merged dataset used for analysis. As shown in Fig. 3b, merging the datasets resulted in a substantial reduction in the number of patients—to 1,422 patients with a 24-month observation window (which proved optimal in subsequent analyses) and 1,355 patients with a 30-month observation window. This reduction is mainly due to excluding patients who only had either claims or clinical data, resulting in a smaller but more comprehensive dataset for analysis.

Table 1 summarizes the demographic, comorbidity, claims-driven, and clinical-driven characteristics of the patient cohort, comprising 1,422 patients; 86 progressed to ESRD (6%), 1,336 did not. For patients who progressed to ESRD, the mean time from CKD stage 3 to ESRD was 4.82 ± 1.82 years. The distribution plot of progression times is provided in Supplementary Figure 1. Patients who progressed to ESRD were significantly younger (69.13 vs. 72.04 years, $p < 0.001$), with notable racial disparities. African American patients were more likely to progress to ESRD (14.0% vs. 4.5%), while White patients had lower progression rates (81.4% vs. 93.0%, $p < 0.001$).

Comorbidities such as hypertension were prevalent in both groups (99%), but diabetes was more frequent in the ESRD group (73.3% vs. 59.0%, $p = 0.009$). Secondary hyperparathyroidism and conduction/dysrhythmias were also significantly higher in ESRD patients ($p < 0.001$ and $p = 0.005$, respectively). In claims-driven features, ESRD patients showed slightly higher counts of outpatient and professional claims ($p = 0.039$) but no significant differences in costs. Clinical-driven features highlighted lower eGFR (17.21 vs. 22.78, $p < 0.001$), lower hemoglobin levels (12.15 vs. 14.25, $p < 0.001$), and higher occurrences of advanced CKD stages in the ESRD group. These differences underscore the clinical and demographic factors associated with ESRD progression.

Table 1: Data characteristics of the patient cohort for analysis

Characteristics	Missing data (%)	Progressed to ESRD (n = 86)	Non-progressed to ESRD (n = 1,336)	P-value
Demographic				
Age (years)	0	69.13 ± 12.37	72.04 ± 11.25	<0.001
Female	0	40 (46.5%)	721 (54.0%)	0.2149
Race	0			<0.001
White		70 (81.4%)	1242 (93.0%)	
African American		12 (14.0%)	60 (4.5%)	
Others		4 (4.6%)	34 (2.5%)	
BMI	4	28.40 ± 5.32	26.40 ± 6.20	<0.001
Comorbidities				
Hypertension	0	85 (99%)	1,323 (99%)	0.863
Diabetes	0	63 (73.3%)	788 (59.0%)	0.009
Anemia	0	55 (64.0%)	828 (62.0%)	0.714
Metabolic acidosis	0	22 (25.6%)	240 (18.0%)	0.077
Proteinuria	0	11 (12.8%)	227 (17.0%)	0.312
Secondary hyperparathyroidism	0	28 (32.6%)	240 (18.0%)	<0.001
Phosphatemia	0	4 (4.7%)	40 (3.0%)	0.39
Heart failure	0	6 (7.0%)	120 (9.0%)	0.526
Stroke	0	1 (1.2%)	40 (3.0%)	0.506
Conduction & dysrhythmias	0	4 (4.7%)	214 (16.0%)	0.005
Claims-driven features				
Count of pharmacy claims	0	120 ± 94	109 ± 86	0.293
Count of inpatient claims	0	3.85 ± 3.41	3.74 ± 3.62	0.773
Count of outpatient claims	0	27.78 ± 24.75	22.07 ± 19.13	0.039
Count of professional claims	0	105.37 ± 77.56	87.43 ± 68.02	0.039
Net cost of pharmacy claims	0	12053 ± 11596	10440 ± 20662	0.242
Net cost of inpatient claims	0	33909 ± 53540	29440 ± 32541	0.446
Net cost of outpatient claims	0	9354 ± 17522	8554 ± 17492	0.682
Net cost of professional claims	0	15512 ± 18657	11640 ± 12748	0.061
Range of claims costs	0	11352 ± 32606	8852 ± 11550	0.481
Standard deviation of claims costs	0	831 ± 1263	757 ± 806	0.593
Clinical-driven features				
eGFR	0	17.21 ± 5.46	22.78 ± 5.66	<0.001
Hemoglobin	3	12.15 ± 2.19	14.25 ± 1.8	<0.001
Bicarbonate	9	22.9 ± 6.36	25.3 ± 4.22	0.001
Serum calcium	6	9.39 ± 3.62	10.21 ± 2.86	0.042
Phosphorus	13	3.61 ± 0.87	3.52 ± 0.72	0.350
CKD stage 3 duration	0	3.7 ± 0.6	3.9 ± 1.4	0.0009
Occurrence of CKD stage 4	0	47 (54.7%)	298 (22.3%)	<0.001
Occurrence of CKD stage 5	0	42 (48.8%)	277 (20.7%)	<0.001
Number of emergency department visits	16	2.63 ± 2.18	2.01 ± 1.99	0.005

5.2 Performance Comparison of Models Across Datasets

To facilitate comprehension of model performance across different data sources, we present results using a 24-month observation window, which yielded optimal performance across most models. Table 2 compares the predictive performance of traditional machine learning and deep learning models across three scenarios: claims data-only, clinical data-only, and merged data.

The results demonstrate several key findings across the different data sources. In the claims data-only scenario, deep learning models, particularly LSTM (AUROC: 0.92, F1: 0.54) and GRU (AUROC: 0.92, F1: 0.50), substantially outperformed traditional machine learning approaches such as logistic regression (AUROC: 0.72, F1: 0.33) and random forest (AUROC: 0.74, F1: 0.36). For clinical data, while the performance gap narrowed, deep learning models maintained their advantage, with LSTM achieving the highest performance (AUROC: 0.88, F1: 0.60). Most notably, the merged dataset combining both claims and clinical data yielded the best overall performance, with LSTM achieving better results across all metrics (AUROC: 0.93, F1: 0.65, AUPRC: 0.61). Comprehensive results across all models and observation windows are provided in Supplementary Table 1.

5.3 Key Feature Analysis Using Explainable AI Techniques

Having identified the 24-month observation window as optimal and LSTM as the best-performing model for ESRD prediction, we employed two complementary explainable AI techniques to understand the features driving these predictions. At the cohort level, we utilized XGBoost's feature importance analysis to identify key predictive variables across the population. At the individual level, we applied SHAP analysis to provide detailed, patient-specific insights into model predictions.

5.3.1 Cohort-Level Key Feature Identification

Our feature importance analysis of the optimal ML model, XGBoost, revealed several key predictors for ESRD progression (see Fig. 4a). The most critical feature was the presence of stage 5 CKD (S5), aligning with clinical literature and expert feedback on its importance in predicting ESRD. Claims-related features, such as the number of outpatient claims (n_claims_O) and total inpatient claim expenses (net_exp_I), also ranked highly. The diverse types of top-ranked features underscore the benefit of multi-sourced data integration, enhancing the model's predictive power. This combination of clinical and claims data not only improves the accuracy of the predictions but also supports more comprehensive and reliable decision-making in clinical practice. However, while XGBoost's feature importance reflects the absolute contribution of each feature, it does not specify whether the influence is positive or negative.

Table 2: Model performance for prediction of ESRD, using claims data-only, clinical data-only, and merged data.

(a) Model performance for prediction of ESRD by using claims data.

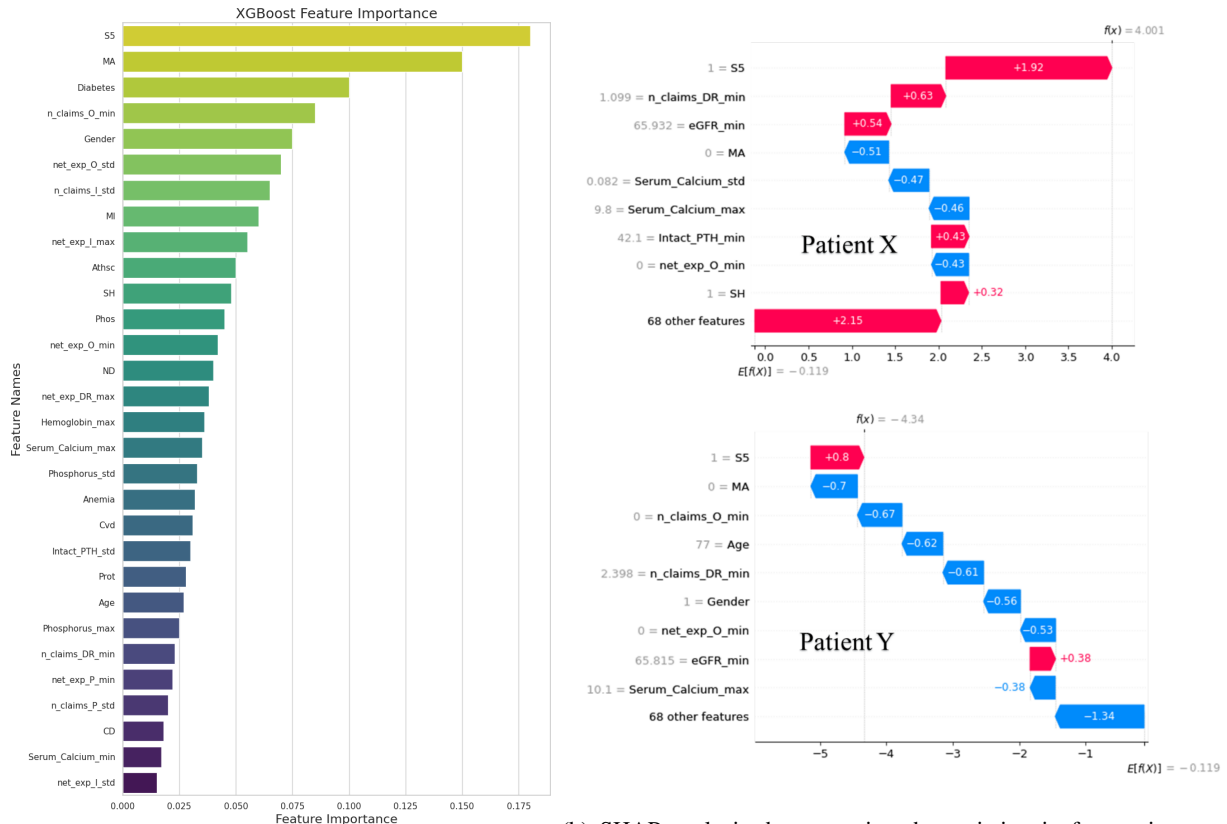
Model	Model performance metric		
	F1 Score	AUROC	AUPRC
Logistic Regression	0.33	0.72	0.44
Random Forest	0.36	0.74	0.48
XGBoost	0.39	0.75	0.47
CNN	0.45	0.82	0.50
RNN	0.50	0.90	0.52
LSTM	0.54	0.92	0.55
GRU	0.50	0.92	0.53
TCN	0.52	0.88	0.53

(b) Model performance for prediction of ESRD by using clinical data.

Model	Model performance metric		
	F1 Score	AUROC	AUPRC
Logistic Regression	0.54	0.76	0.47
Random Forest	0.58	0.79	0.51
XGBoost	0.57	0.80	0.52
CNN	0.56	0.84	0.53
RNN	0.61	0.85	0.53
LSTM	0.60	0.88	0.56
GRU	0.60	0.87	0.55
TCN	0.61	0.83	0.54

(c) Model performance for prediction of ESRD by using merged data.

Model	Model performance metric		
	F1 Score	AUROC	AUPRC
Logistic Regression	0.55	0.75	0.45
Random Forest	0.60	0.84	0.49
XGBoost	0.61	0.85	0.51
CNN	0.56	0.80	0.46
RNN	0.62	0.87	0.53
LSTM	0.65	0.93	0.61
GRU	0.63	0.90	0.58
TCN	0.61	0.89	0.58



(a) Top 30 features of importance for the XGBoost model. ESRD risk prediction for two patients with CKD Stage 5.

(b) SHAP analysis demonstrating the variation in feature impact on ESRD risk prediction for two patients with CKD Stage 5.

Figure 4: Key Feature Analysis: Feature importance and SHAP analysis for ESRD risk prediction using a 24-month observation window.

5.3.2 Feature Impact at the Individual Patient Level Using SHAP Analysis

While the previous subsection explored feature importance at the cohort level, the uniqueness of each patient's condition necessitates a more personalized approach. To aid healthcare providers in making tailored decisions, we applied SHAP analysis to identify the key features driving individual patient predictions.

We present SHAP force plots for two patients, Patient X and Patient Y, both of whom were correctly predicted for their risk of progressing to ESRD. Despite both having CKD Stage 5, they showed notably different patterns of contributing features, highlighting how the same clinical outcome can arise from distinct combinations of risk factors and underscoring the importance of personalized treatment strategies.

In Figure 4b, features increasing ESRD risk are highlighted in red, while those reducing risk are in blue. For Patient X, factors such as Stage 5 CKD (S5) and a high number of outpatient claims (`n_claims_DR_min`) elevated the risk, while higher eGFR levels and the absence of certain markers reduced it. For Patient Y, lower risk was driven by factors such as younger age, fewer minimum inpatient claims (`net_exp_O_min`), and lower minimum eGFR values, despite also having a Stage 5 CKD diagnosis (S5).

This variation in key features, even among patients with the same CKD stage, highlights the importance of aiding the identification of individual differences in treatment planning. SHAP analysis offers a clear visualization of these factors, enabling healthcare providers to tailor interventions to each patient's unique risk profile and modifiable factors.

5.4 Analysis of Model Misclassifications: Type I and Type II Errors

To explore these misclassifications, we analyzed Type I and Type II errors, as depicted in Figure 5. Notably, most incorrect predictions for patients who progressed to ESRD, yet were predicted otherwise, cluster near the lower end of the plot rather than around the 0.5 decision threshold or randomly scattered. This clustering suggests consistent factors may be influencing these errors, warranting a deeper investigation.

To understand the underlying causes of model misclassification, we conducted a detailed analysis of Type I and Type II errors. We focused particularly on Type II errors, where patients were incorrectly predicted not to develop ESRD but ultimately did progress to the condition. By comparing the 16 false negatives (patients shown in the lower part of the right plot) with the 70 true positives (patients correctly predicted to progress to ESRD, shown in the upper part of the right plot), we aimed to identify patterns and characteristics that might explain why the model failed to identify these high-risk patients. These errors can delay essential treatment, potentially accelerating disease progression.

Conversely, Type I errors represent patients who were incorrectly predicted to develop ESRD but did not actually progress. Our analysis contrasted 17 false positives (patients shown in the upper part of the left plot) with 1,319 true

negatives (patients correctly predicted not to progress, shown in the lower part of the left plot). These Type I errors are particularly concerning in clinical practice as they could lead to unnecessary medical interventions and inefficient allocation of healthcare resources, potentially diverting attention from patients at genuine risk of ESRD progression. Understanding the characteristics distinguishing these misclassified cases from correctly predicted ones may provide valuable insights for model refinement and improved clinical decision support.

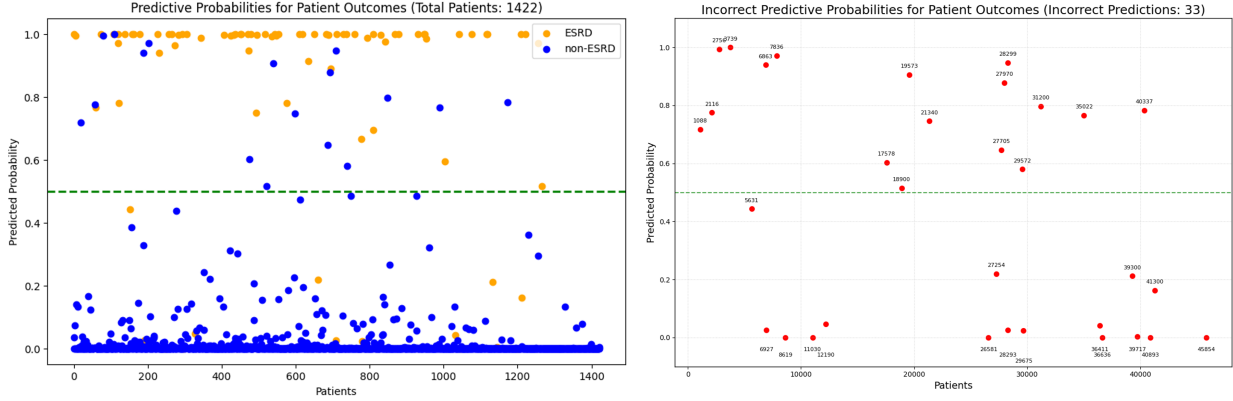


Figure 5: Analysis of Model Misclassification: Type I and Type II Errors. The left plots illustrate the predicted probability distribution for all patient outcomes, highlighting the model’s performance across the dataset. The right plots focus on the incorrectly predicted cases, distinguishing between Type I errors (false positives) and Type II errors (false negatives).

Based on Table 3a, CKD Stage 5 emerges as a critical feature. For patients incorrectly predicted as not progressing to ESRD (false negatives), the mean value for CKD Stage 5 at timestamp 6 is 0.06, which is significantly lower than the 0.36 mean for those correctly predicted to progress. This suggests that these patients did not have a Stage 5 record until the subsequent timestamp. The model likely interpreted the absence of a Stage 5 indicator up to timestamp 7 as a sign that ESRD development was unlikely. However, after consulting with nephrologists and examining the literature on CKD progression, we note that some CKD patients may experience a sudden decline in kidney function, "crashing" into dialysis, where they appear stable for a period before rapidly progressing to ESRD due to acute kidney injury or treatments during hospitalization.

Based on Table 3b, CKD Stage 5 appears in both timestamps 6 and 7 for the incorrectly predicted group, indicating that these patients had Stage 5 records at these timestamps but did not actually progress to ESRD. This is unusual. One possible explanation could be the issue of data censoring. Our dataset spans from 2009 to 2018, so patients incorrectly predicted to develop ESRD, with continuous Stage 5 records, might have progressed to ESRD in 2019 or later. Additional data collection beyond 2018 would be needed to update and refine this analysis.

Table 3: Analysis of Type I and Type II Errors: Features and Their Impact on Prediction Accuracy. This table presents representative subsets of features under various timestamps. Features in bold appear in both analyses.

(a) Type II Error Analysis: Feature Comparison Between False Negatives and True Positives.

Model	Mean		P-value	Timestamp
	Correct	Incorrect		
n_claims_I	0.70	0.14	0.048752	5
n_claims_O	5.71	2.67	0.001325	2
net_exp_O	3831.83	830.61	0.002747	0
S5	0.36	0.06	0.001189	6
S5	0.37	0.49	0.662073	7
net_exp_O	4219.01	1044.37	0.001883	4

(b) Type I Error Analysis: Feature Comparison Between False Positives and True Negatives.

Model	Mean		P-value	Timestamp
	Correct	Incorrect		
n_claims_DR	13.52	7.21	0.001156	3
n_claims_O	3.03	1.69	0.009384	4
S4	3831.83	830.61	0.002747	4
S5	0.09	0.35	0.000250	6
S5	0.08	0.35	0.001388	7
net_exp_O	1044.82	333.61	0.000324	4

5.5 Impact of Updated eGFR Equation on Racial Bias in Predictions

When comparing predictions between the 2009 and 2021 eGFR equations (Fig 6a, 6b), we observed a decrease in total incorrect predictions from 33 to 28, reducing the overall error rate from 0.0232 to 0.0228. Among these misclassifications, only 7 cases were common to both equations. Analysis of racial distribution in prediction errors (Fig 6c, 6d) revealed varying patterns across different groups: incorrect predictions for white patients increased from 2 to 4, African American patients decreased from 4 to 1, and patients in the "Other" category increased from 10 to 12. The demographic breakdown for the 2021 equation cohort, including race, gender, and ESRD outcomes, is shown in Fig 6c. However, these numbers are clearly too small for robust insights.

6 Discussion

This study demonstrates the value of integrating multiple data sources and deep learning methodologies for improving ESRD progression predictions in CKD patients. By combining claims and EHR data with LSTM and GRU models, which excel at capturing temporal dependencies, we achieved enhanced predictive accuracy using a 24-month observation window. This window length provides an optimal balance between early detection and prediction reliability, supporting timely clinical interventions. Our research addresses a critical gap in chronic disease management by integrating clinical and claims data, offering a more comprehensive view of patient health trajectories than single-source

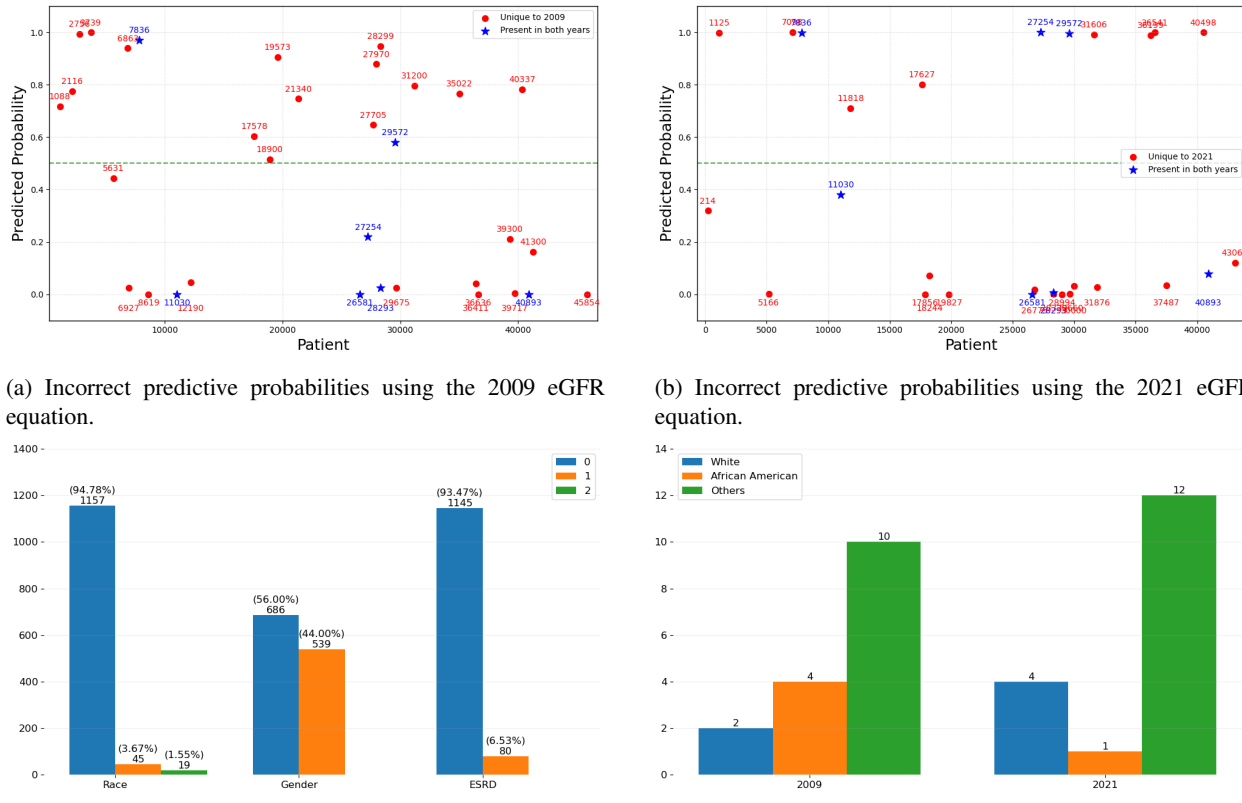


Figure 6: Impact of Updated eGFR Equations (2009 vs. 2021) on Prediction Errors and Racial Bias. Subplots (a) and (b) compare incorrect predictions using the two eGFR equations, while (c) and (d) explore the demographic distribution and racial disparities among incorrectly predicted patients.

approaches. The combination of medical indicators and healthcare utilization patterns provides deeper insights into ESRD progression risk factors, making the model more robust across diverse patient populations. The determination of this optimal observation window represents a significant advancement in balancing timely interventions with prediction accuracy, enabling healthcare providers to efficiently monitor CKD progression while minimizing data collection burden.

Our findings suggest that while the updated 2021 eGFR equation shows modest improvement in overall prediction accuracy compared to the 2009 equation (error rate reduction from 0.0232 to 0.0228) in this study population, the more useful insight may come from the pattern of misclassifications. The fact that only 7 cases were misclassified by both equations, despite similar overall error rates, indicates that these equations capture different aspects of kidney function and disease progression. This has important implications for clinical practice: while the 2021 equation may better serve minoritized populations by removing race-based adjustments, the persistence of prediction errors clustered in certain patient profiles suggests that eGFR alone may not be sufficient for accurate ESRD prediction. These findings underscore the need for a multi-faceted approach to risk assessment, combining both traditional clinical markers and novel predictive features. By leveraging integrated data sources and advanced modeling techniques, healthcare providers can develop more comprehensive risk assessment strategies, potentially leading to more targeted interventions and improved patient outcomes across diverse populations.

6.1 Limitations

Our study's reliance on data from a single institution limits the model's generalizability to all care delivery settings. Incorporating data from more sources could enhance robustness and applicability across different clinical settings. The framework is also currently tailored to predict ESRD outcomes specifically in CKD patients; expanding it to other chronic diseases could provide broader insights.

The use of EHR data presents challenges, such as observational bias, incomplete data, and underrepresentation of certain populations, which can impact model accuracy and fairness. Addressing these issues through comprehensive datasets or advanced imputation techniques is necessary for further improving prediction reliability.

Despite employing data oversampling methods, the disparity between our model's high AUROC scores and relatively lower F1 and AUPRC scores indicates persistent challenges in addressing data imbalance. This gap suggests that traditional oversampling techniques may not fully compensate for the inherent imbalance in ESRD progression data. To enhance performance, exploring advanced data balancing methods is essential. Techniques such as ensemble methods, cost-sensitive learning, and hybrid approaches that combine oversampling and undersampling have shown

promise in effectively managing imbalanced datasets.

Additionally, the model does not fully account for time lags between claims and clinical data, which may affect the precision of predictions. Reducing these discrepancies is essential for enhancing the model's effectiveness in clinical practice.

6.2 Future Directions

Addressing Data Censoring: To mitigate data censoring issues, an initial strategy could involve truncating the data up to 2016 and analyzing patient outcomes in 2017 and 2018. Following this, expanding the dataset to include more recent patient information beyond 2018 would be crucial. This expansion would enhance our understanding of health trajectories and disease progression, enabling continuous refinement of the model to better align with evolving healthcare practices and patient demographics.

Integration of Unstructured Clinical Notes: Future model iterations will integrate unstructured clinical notes, such as physician narratives and discharge summaries, to capture detailed patient information often missed in structured formats. This approach aims to provide a more comprehensive view of patient health, enhancing outcome predictions and enabling more personalized interventions.

Advanced Methods for Time-Lag Mitigation: Advanced techniques to mitigate time lags between claims and clinical data, such as algorithms that adjust for expected delays or incorporate more real-time data sources for more accurate triangulation, are needed to improve the model's ability to handle these temporal discrepancies, enhance prediction accuracy and ensure timely, data-driven interventions.

Expansion to Other Chronic Diseases: To evaluate framework's versatility, we plan to apply it to other chronic conditions, such as heart disease. This will help assess its applicability across various care delivery settings, providing insights into its broader potential for chronic disease management and informing further optimization efforts.

7 Conclusion

As multiple sources of patient-level healthcare data continue to get integrated and analyzed in large data repositories and cloud computing platforms, this study presents an insightful illustrative approach for predicting ESRD outcome in CKD patients by integrating clinical and claims data with advanced machine learning and deep learning methods. Our results demonstrate that this combined data strategy significantly improves prediction accuracy, offering a more holistic understanding of CKD progression. Through explainable AI techniques such as SHAP analysis, we identified critical factors influencing predictions at both individual and cohort levels.

A key contribution of this work is the development of a framework that optimizes the observation window, balancing early detection with predictive accuracy to enhance clinical decision-making. The 24-month observation window was identified as the optimal period for maximizing prediction effectiveness while minimizing unnecessary interventions.

Additionally, our assessment of the updated 2021 eGFR equation highlights an approach to health equity, contributing to fairer healthcare outcomes.

Overall, this study advances chronic disease management by utilizing integrated data and innovative AI techniques, paving the way for more accurate, personalized, and equitable care in CKD management. These findings lay the groundwork for future research to refine predictive models and expand their application to other chronic diseases.

8 Acknowledgments

The authors sincerely thank the community nephrology practice for providing access to their de-identified clinical data and the wealth of medical knowledge and inputs shared by several nephrologists in the practice and their CIO on the raw data and the results of our analysis. Similarly, we are very grateful to the health insurance organization for providing access to the de-identified claims data on their shared set of patients with the nephrology practice and for the invaluable help provided by their data team in understanding the claims data.

AI Writing Assistance: All drafts of this manuscript were created by the authors without AI assistance. GPT-4o and Claude 3.5 (Sonnet) were used solely for polishing grammar and refining expression. The outputs from these tools were critically compared and reviewed by the authors to ensure accuracy and clarity. Final revisions were made by the authors to ensure all expressions align with the intended meaning and academic standards.

Funding Statement

This work was supported by the fellowship support for Y.L. from the Center for Machine Learning and Health (CMLH) at Carnegie Mellon University.

Competing Interests Statement

The authors have no competing interests to declare.

Data Availability Statement

The data underlying this article consist of active healthcare clinical and claims data, which cannot be shared publicly due to privacy regulations and the sensitive nature of the information.

References

1. Foundation NK. Chronic Kidney Disease (CKD). National Kidney Foundation. 2024. Available from: <https://www.kidney.org/atoz/content/about-chronic-kidney-disease>.
2. Lin CM, Yang MC, Hwang SJ, Sung JM. Progression of stages 3b–5 chronic kidney disease—preliminary results of Taiwan National pre-ESRD disease management program in Southern Taiwan. *Journal of the Formosan Medical Association*. 2013;112(12):773-82.
3. for Health Statistics NC. Mortality in the United States. <https://www.cdc.gov/nchs/products/databriefs/db395.htm>. 2019.
4. Guo Y, Yu H, Chen D, Zhao YY. Machine learning distilled metabolite biomarkers for early stage renal injury. *Metabolomics*. 2020;16(1):1-10.
5. Belur Nagaraj S, Pena MJ, Ju W, Heerspink HL, Consortium BD. Machine-learning-based early prediction of end-stage renal disease in patients with diabetic kidney disease using clinical trials data. *Diabetes, Obesity and Metabolism*. 2020;22(12):2479-86.
6. Krishnamurthy V, Gopal A, Kannan R, et al. Machine learning for predicting outcomes in chronic kidney disease: Challenges and opportunities. *IEEE Journal of Biomedical and Health Informatics*. 2021;25(4):1319-31.
7. Li Y, Al-Sayouri S, Padman R. Towards Interpretable End-Stage Renal Disease (ESRD) Prediction: Utilizing Administrative Claims Data with Explainable AI Techniques. *arXiv preprint arXiv:240912087*. 2024.
8. Sharma A, Alvarez PJ, Woods SD, Dai D. A Model to Predict Risk of Hyperkalemia in Patients with Chronic Kidney Disease Using a Large Administrative Claims Database. *ClinicoEconomics and Outcomes Research: CEOR*. 2020;12:657.
9. Tangri N, Stevens LA, Griffith J, Tighiouart H, Djurdjev O, Naimark D, et al. A predictive model for progression of chronic kidney disease to kidney failure. *JAMA*. 2011;305(15):1553-9.
10. Foundation NK, . Estimated Glomerular Filtration Rate (eGFR). National Kidney Foundation; n.d. Accessed: 2024-12-16. <https://www.kidney.org/kidney-topics/estimated-glomerular-filtration-rate-egfr>.
11. Sun L, Shang J, Xiao J, Zhao Z. Development and validation of a predictive model for end-stage renal disease risk in patients with diabetic nephropathy confirmed by renal biopsy. *PeerJ*. 2020;8:e8499.
12. Lundberg SM, Lee SI. A unified approach to interpreting model predictions. *Advances in neural information processing systems*. 2017;30.
13. Ribeiro MT, Singh S, Guestrin C. “Why should I trust you?”: Explaining the predictions of any classifier. In: *Proceedings of the 22nd ACM SIGKDD international conference on knowledge discovery and data mining*. ACM; 2016. p. 1135-44.

14. van Rijsbergen CJ. Information Retrieval. 2nd ed. Butterworth-Heinemann; 1979. Introduced the F-measure, which includes the F1-score.
15. Hanley JA, McNeil BJ. The meaning and use of the area under a receiver operating characteristic (ROC) curve. *Radiology*. 1982;143(1):29-36.
16. Davis J, Goadrich M. The relationship between Precision-Recall and ROC curves. In: Proceedings of the 23rd International Conference on Machine Learning (ICML). ACM; 2006. p. 233-40.
17. White IR, Royston P, Wood AM. Multiple imputation using chained equations: issues and guidance for practice. *Statistics in medicine*. 2011;30(4):377-99.
18. Sedgwick P. Log transformation of data. *BMJ*. 2012;345.
19. Aryal S. Anomaly Detection Technique Robust to Units and Scales of Measurement. In: Advances in Knowledge Discovery and Data Mining (PAKDD 2018). Springer; 2018. p. 589-601. Available from: https://link.springer.com/chapter/10.1007/978-3-319-93034-3_47.
20. Foundation NK, . Urine Albumin-to-Creatinine Ratio (UACR). National Kidney Foundation; n.d. Accessed: 2024-12-16. <https://www.kidney.org/kidney-topics/urine-albumin-creatinine-ratio>.
21. Chawla NV, Bowyer KW, Hall LO, Kegelmeyer WP. SMOTE: Synthetic Minority Over-sampling Technique. *Journal of Artificial Intelligence Research*. 2002;16:321-57. Available from: <https://www.jair.org/index.php/jair/article/view/10302>.
22. Saif D, Sarhan AM, Elshennawy NM. Early prediction of chronic kidney disease based on ensemble of deep learning models and optimizers. *Journal of electrical systems and information technology*. 2024;11(1):17.
23. Kleinbaum DG, Klein M. Logistic Regression: A Self-Learning Text. 3rd ed. Springer Science & Business Media; 2010.
24. Breiman L. Random Forests. *Machine Learning*. 2001;45(1):5-32.
25. Chen T, Guestrin C. XGBoost: A Scalable Tree Boosting System. *Proceedings of the 22nd ACM SIGKDD International Conference on Knowledge Discovery and Data Mining*. 2016:785-94.
26. Wong TT, Yeh PY. Reliable accuracy estimates from k-fold cross validation. *IEEE Transactions on Knowledge and Data Engineering*. 2019;32(8):1586-94.
27. Burckhardt P, Nagin D, Padman R. Multi-Trajectory Models of Chronic Kidney Disease Progression. *AMIA Annu Symp Proc*. 2017:1737-46.
28. LeCun Y, Bengio Y, Hinton G. Deep learning. *Nature*. 2015;521(7553):436-44.
29. Rumelhart DE, Hinton GE, Williams RJ. Learning representations by back-propagating errors. *Nature*. 1986;323(6088):533-6.

30. Hochreiter S, Schmidhuber J. Long short-term memory. *Neural computation*. 1997;9(8):1735-80.
31. Cho K, Van Merriënboer B, Gulcehre C, Bahdanau D, Bougares F, Schwenk H, et al. Learning phrase representations using RNN encoder-decoder for statistical machine translation. In: Proceedings of the 2014 Conference on Empirical Methods in Natural Language Processing (EMNLP). Association for Computational Linguistics; 2014. p. 1724-34.
32. Bai S, Kolter JZ, Koltun V. An empirical evaluation of generic convolutional and recurrent networks for sequence modeling. *arXiv preprint arXiv:180301271*. 2018.
33. Raschka S. Model evaluation, model selection, and algorithm selection in machine learning. *arXiv preprint arXiv:181112808*. 2018.
34. ai H. h2o: Python Interface for H2O. H2O.ai; 2022. Python package version 3.42.0.2. Available from: <https://github.com/h2oai/h2o-3>.
35. Microsoft. Neural Network Intelligence (NNI). Microsoft; 2024. Available at <https://github.com/microsoft/nni>.
36. Inker LA, Eneanya ND, Coresh J, Tighiouart H, Wang D, Sang Y, et al. New creatinine-and cystatin C-based equations to estimate GFR without race. *New England Journal of Medicine*. 2021;385(19):1737-49.
37. Miller WG, Kaufman HW, Levey AS, Straseski JA, Wilhelms KW, Yu HY, et al. National Kidney Foundation Laboratory Engagement Working Group recommendations for implementing the CKD-EPI 2021 race-free equations for estimated glomerular filtration rate: practical guidance for clinical laboratories. *Clinical chemistry*. 2022;68(4):511-20.
38. Levey AS, Titan SM, Powe NR, Coresh J, Inker LA. Kidney disease, race, and GFR estimation. *Clinical Journal of the American Society of Nephrology*. 2020;15(8):1203-12.
39. Diao JA, Inker LA, Levey AS, Tighiouart H, Powe NR, Crews DC, et al. Clinical implications of removing race from estimates of kidney function. *JAMA*. 2021;325(2):184-96.

Supplementary

Supplementary Table 1: Model Performance Metrics Across Observation Windows

Table 4: Comparison of AUROC and F1 scores across different models, using claims data-only, clinical data-only, and merged data. Bold font is used to mark the best performance within each category (ML or DL methods), while bold and italic font highlights the best overall performance across all methods (ML + DL).

(a) Performance of models using claims data only.

		Model/Metrics	6 months		12 months		18 months		24 months		30 months	
			AUC	F1	AUC	F1	AUC	F1	AUC	F1	AUC	F1
Claims Data Only Modeling	Machine Learning Methods	Logistic Regression	0.61	0.24	0.64	0.31	0.70	0.32	0.72	0.33	0.71	0.29
		Random Forest	0.69	0.26	0.73	0.33	0.74	0.41	0.74	0.36	0.68	0.33
		XGBoost	0.70	0.27	0.75	0.35	0.78	0.42	0.75	0.39	0.69	0.38
	Deep Learning Methods	CNN	0.72	0.36	0.73	0.42	0.81	0.44	0.82	0.45	0.84	0.44
		RNN	0.77	0.39	0.75	0.44	0.83	0.49	0.90	0.50	0.82	0.47
		LSTM	0.76	0.33	0.79	0.43	0.86	0.45	0.92	0.54	0.87	0.44
		GRU	0.70	0.34	0.78	0.46	0.88	0.45	0.91	0.50	0.86	0.42
		TCN	0.72	0.36	0.81	0.37	0.85	0.46	0.88	0.52	0.85	0.43

(b) Performance of models using clinical data only.

		Model/Metrics	6 months		12 months		18 months		24 months		30 months	
			AUC	F1	AUC	F1	AUC	F1	AUC	F1	AUC	F1
Clinical Data Only Modeling	Machine Learning Methods	Logistic Regression	0.63	0.46	0.70	0.49	0.76	0.51	0.76	0.54	0.75	0.53
		Random Forest	0.70	0.53	0.76	0.53	0.80	0.58	0.79	0.58	0.77	0.54
		XGBoost	0.73	0.52	0.76	0.55	0.80	0.59	0.80	0.57	0.72	0.55
	Deep Learning Methods	CNN	0.73	0.51	0.75	0.54	0.80	0.55	0.84	0.56	0.80	0.52
		RNN	0.74	0.53	0.77	0.57	0.82	0.60	0.85	0.61	0.79	0.55
		LSTM	0.77	0.54	0.78	0.56	0.84	0.63	0.88	0.60	0.82	0.57
		GRU	0.80	0.54	0.77	0.57	0.83	0.61	0.87	0.60	0.84	0.53
		TCN	0.72	0.50	0.73	0.53	0.80	0.57	0.83	0.61	0.81	0.55

(c) Performance of models using merged data.

		Model/Metrics	6 months		12 months		18 months		24 months		30 months	
			AUC	F1	AUC	F1	AUC	F1	AUC	F1	AUC	F1
Merged Data Modeling	Machine Learning Methods	Logistic Regression	0.65	0.46	0.69	0.47	0.76	0.54	0.75	0.55	0.78	0.54
		Random Forest	0.74	0.44	0.77	0.52	0.83	0.58	0.84	0.60	0.80	0.55
		XGBoost	0.73	0.45	0.76	0.50	0.82	0.58	0.85	0.61	0.82	0.59
	Deep Learning Methods	CNN	0.70	0.45	0.76	0.46	0.77	0.55	0.80	0.56	0.82	0.55
		RNN	0.75	0.51	0.80	0.58	0.86	0.60	0.87	0.62	0.85	0.61
		LSTM	0.76	0.53	0.84	0.59	0.93	0.63	0.93	0.65	0.84	0.59
		GRU	0.75	0.51	0.76	0.56	0.91	0.62	0.90	0.63	0.86	0.57
		TCN	0.71	0.49	0.74	0.57	0.88	0.60	0.89	0.61	0.91	0.59

Supplementary Figure 1

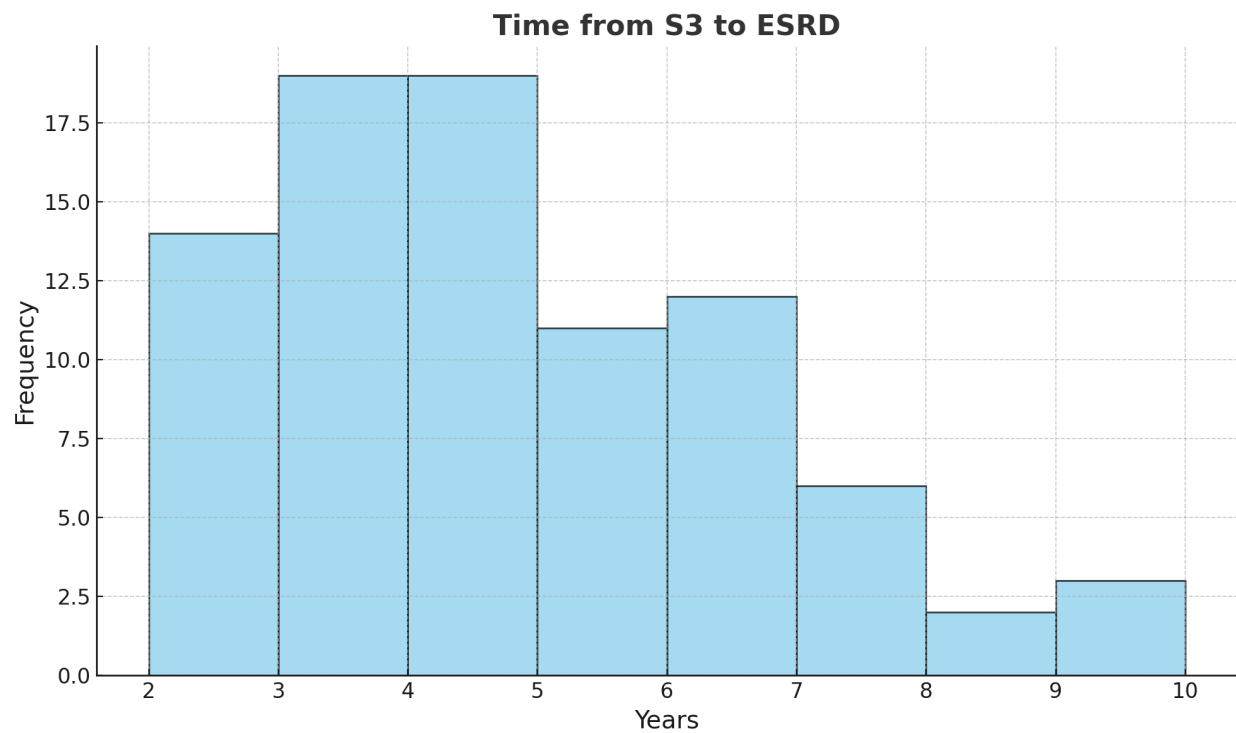


Figure 7: Distribution of time to ESRD for the ESRD cohort. The plot illustrates the variability in time to ESRD across the cohort, with a mean time of 4.82 years and a standard deviation of 1.82 years.

Supplementary Table 2

Table 5: Mapping between Feature Abbreviations in The Feature Importance Plot and Full Names

Short Name	Full Name
S5	Serum Albumin
MA	Metabolic Acidosis
Diabetes	Diabetes
n_claims_O_min	Number of Outpatient Claims (Min)
Gender	Gender
net_exp_O_std	Net Expense for Outpatient Claims (Std Dev)
n_claims_I_std	Number of Inpatient Claims (Std Dev)
MI	Myocardial Infarction
net_exp_I_max	Net Expense for Inpatient Claims (Max)
Athsc	Atherosclerosis
SH	Secondary Hyperparathyroidism
Phos	Phosphatemia
net_exp_O_min	Net Expense for Outpatient Claims (Min)
ND	Nutritional Disorders
net_exp_DR_max	Net Expense for Drug-Related Claims (Max)
Hemoglobin_max	Hemoglobin Level (Max)
Serum_Calcium_max	Serum Calcium Level (Max)
Phosphorus_std	Phosphorus Level (Std Dev)
Anemia	Anemia Diagnosis
Cvd	Cardiovascular Disease
IntactPTH_std	Intact Parathyroid Hormone (Std Dev)
Prot	Proteinuria
Age	Age
Phosphorus_max	Phosphorus Level (Max)
n_claims_DR_min	Number of Drug-Related Claims (Min)
net_exp_P_min	Net Expense for Pharmacy Claims (Min)
n_claims_P_std	Number of Pharmacy Claims (Std Dev)
CD	Conduction & Dysrhythmias
Serum_Calcium_min	Serum Calcium Level (Min)
net_exp_I_std	Net Expense for Inpatient Claims (Std Dev)